A Model of Anatomically Opposed Ischaemia

Peter R Johnston

Griffith University, Nathan, Queensland, Australia

Abstract

This study aims to gain an understanding of anatomically opposed ischaemia, or "ischaemic ST-segment counterpoise", by determining and examining epicardial potential distributions resulting from two regions of subendocardial ischaemia during the ST-segment.

The finite volume method is used to solve the passive bidomain equation in an isolated semi-ellipsoidal model of the left ventricle. A model with one moderately sized ischaemic region is used as a base case. Subsequently, regions of ischaemia of varying size are placed in various positions in the posterior and anterior, inferior or left lateral regions of the ventricular wall.

Simulations show that having two regions of ischaemia produces epicardial potential distributions that are different from those with one ischaemic region. With two ischaemic regions of markedly different size within the left ventricular wall, the larger region dominates the resulting epicardial potential distribution, making the smaller region difficult to observe. Two ischaemic regions of similar size are identifiable on the epicardial potential distribution.

1. Introduction

The phenomenon of anatomically opposed ischaemia, or "ischaemic ST-segment counterpoise", is believed to result in a false negative conclusion from an exercise electrocardiogram (ECG) [1–3]. The basis for this conclusion was the contrast between the recording of a normal exercise ECG and subsequent thallium-210 myocardial single-positron emission computerised tomography imaging of the heart showing severe myocardial infarction in the anterior, septal, posteroinferior and posterolateral planes of the heart. Severe stenoses in the left anterior descending and right coronary arteries were also discovered during coronary angiography. The explanation for these contradictory observations was a cancellation effect in ischaemic ST-segment vectors due to equally intensive and extensive ischaemia involving opposite planes of the heart [2].

In order to shed light on these findings, a numerical model of a blood filled left ventricle, in the shape of a half ellipsoid, was constructed. To this model, one or two regions of ischaemic tissue were added at various locations and of varying sizes. Resulting epicardial potential distributions were obtained by solving the governing passive bidomain equation [4] via the finite volume method [5].

Areas of ischaemia were added to the model of the left ventricle at various combinations of right, left, anterior, posterior and inferior regions of the heart. As a baseline, only one ischaemic region of moderate size was used. With two ischaemic regions present, the relative sizes of the ischaemic regions ranged from being equal to one region being significantly larger than the other. The resulting epicardial potential distributions are discussed in Section 3.

2. Methods

Governing Equations: The passive bidomain equation, which governs the electric potential in a region of cardiac tissue during the ST segment of the electrocardiogram, is given by [4]

$$\nabla \cdot (\mathbf{M_i} + \mathbf{M_e}) \nabla \phi_e = -\nabla \cdot \mathbf{M_i} \nabla \phi_\mathbf{m} \qquad (1)$$

where ϕ_e is the extracellular potential in the cardiac tissue, ϕ_m is the specified transmembrane potential distribution and $\mathbf{M_i}$ and $\mathbf{M_e}$ represent conductivity tensors for the intracellular (i) and extracellular (e) spaces, respectively. These conductivity tensors contain information about the local fibre direction.

The conductivity tensors take the form [6]

$$\mathbf{M_h} = \mathbf{A} \mathbf{G_h} \mathbf{A^T} \qquad (2)$$

for $h = i$ or e, where $\mathbf{G_h}$ is a diagonal matrix containing the conductivity values along the fibre direction, g_{hl}, across the sheets of fibres, g_{ht}, and between the sheets of fibres, g_{hn}. Here it will be assumed that $g_{ht} = g_{hn}$. The matrix $\mathbf{A} = \{\mathbf{a_{ij}}\}$ is a rotation matrix mapping the local fibre direction into the global coordinate system. Under these assumptions it can be shown that

$$\mathbf{M_h} = \mathbf{g_{ht}} \mathbf{I} + (\mathbf{g_{hl}} - \mathbf{g_{ht}}) \, \hat{\mathbf{a}}^\mathbf{T} \hat{\mathbf{a}} \qquad (3)$$

where $\mathbf{I}$ is the 3×3 identity matrix and $\hat{\mathbf{a}}$ is the unit vector indicating the local direction of the fibres [7].

The ventricular cavity is assumed to be filled with blood where the electric potential, ϕ_b, is governed by Laplace's equation

$$\nabla^2 \phi_b = 0. \tag{4}$$

Model Geometry: For the purposes of this study it will be assumed that the computational domain is represented by a half ellipsoid with a circular cross-section. The semi-major axis of the ellipsoid representing the epicardial surface has a length of 6cm and the two semi-minor axes both have a length of 3cm. The ventricular wall is assumed to be 1cm thick, yielding an inner ellipsoid representing the endocardial surface with semi-major axis of 5cm and semi-minor axes of 2cm, respectively. The origin of the rectangular (x, y, z) coordinate system is placed such that the epicardial surface, Γ_{epi}, of the ventricle is represented by the equation

$$\left(\frac{x}{3}\right)^2 + \left(\frac{y}{3}\right)^2 + \left(\frac{z}{6}\right)^2 = 1$$

for $z \geq 0$. Similarly, the endocardial surface, Γ_{endo}, is represented by the surface

$$\left(\frac{x}{2}\right)^2 + \left(\frac{y}{2}\right)^2 + \left(\frac{z}{5}\right)^2 = 1$$

Also, as mentioned above, the central cavity within the half ellipsoid was filled with blood.

Regions of partial thickness ischaemia, extending from the endocardium towards the epicardium were placed at various positions within the ventricular wall. The regions of ischaemia were parallelepipedal in shape, with sides aligned with the angular coordinate directions of the ellipsoidal coordinate system, as shown in Figure 1.

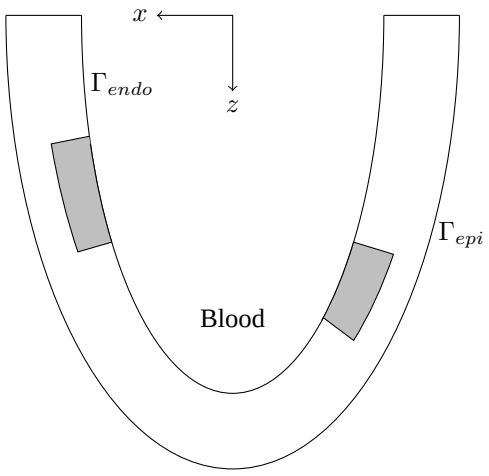

Figure 1. Cross-section of the model of the left ventricle showing two regions of ischaemia (shaded gray) within the cardiac tissue. The regions of ischaemia have limited ranges in the azimuthal direction.

Boundary Conditions: To solve the governing equations, several boundary conditions are required. It will be assumed that the epicardial surface is insulated, i.e.

$$\text{on } \Gamma_{\text{epi}}, \quad \frac{\partial \phi_{\text{e}}}{\partial \mathbf{n}} = 0 \tag{5}$$

where $\mathbf{n}$ is the outward pointing normal to the surface Γ_{epi}. This is chosen to match experimental protocols, where epicardial potentials were measured in an open chest experiment [8]. It will also be assumed that the edges of the tissue and the blood mass on the $x - y$ plane are insulated, that is for $z = 0$

$$\frac{\partial \phi_e}{\partial z} = 0 \quad \text{for} \quad 2 \leq \text{r} \leq 3 \tag{6}$$

$$\frac{\partial \phi_b}{\partial z} = 0 \quad \text{for} \quad 0 \leq \text{r} \leq 2 \tag{7}$$

$$\tag{8}$$

where $r = \sqrt{x^2 + y^2}$. Finally, continuity of potential and current is assumed between the tissue and the blood mass, so on Γ_{endo}

$$\phi_e = \phi_b \quad \text{and} \quad \text{g}_{\text{et}} \frac{\partial \phi_{\text{e}}}{\partial \mathbf{n}} = \text{g}_{\text{b}} \frac{\partial \phi_{\text{b}}}{\partial \mathbf{n}} \tag{9}$$

where g_b is the conductivity of blood.

Parameter Values: The conductivity values used in this study are taken from Clerc [9]: $g_{il} = 1.74$, $g_{el} = 6.25$, $g_{it} = 0.193$ and $g_{et} = 2.36$ (all values are in mS/cm). The conductivity of blood as taken as $g_b = 6.7$ mS/cm [10].

The transition, between the normal and ischaemic tissue, is described by a smooth variation in the transmembrane potential during the ST segment. The difference in plateau transmembrane potential between normal and ischaemic tissue, $\Delta\phi_p$, is set at -30 mV and the transition is described in terms of exponential and hyperbolic functions [11, 12]. In all cases the ischaemic regions cover 50% of the ventricular wall, starting at the endocardium, extending towards the epicardium.

For this study, it will be assumed that fibres rotate through an angle of 120° (chosen for consistency with previous models [12, 13]), moving from the epicardium to the endocardium. The fibres on the epicardium are inclined at an angle of 45° to the positive z-axis.

3. Results

In each of the figures that follow the epicardial potential distribution (EPD) is projected onto a circle with the apex of the ventricle at the centre of the circle, so that the view is from below. The anterior of the ventricle is towards the top of the picture and the left of the ventricle is to the right. Potentials are plotted relative to a kind of Wilson's central terminal, obtained by averaging potentials at the

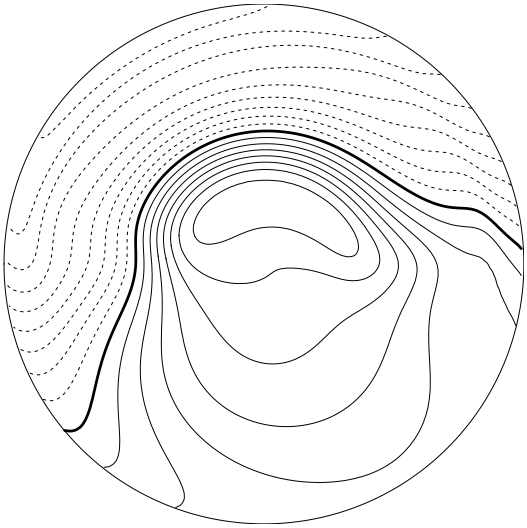

Figure 2. EPD on the surface of the ventricle from one region of subendocardial ischaemia located in the anterior wall of the ventricle. (Min: -1.87mV, Max: 1.52mV)

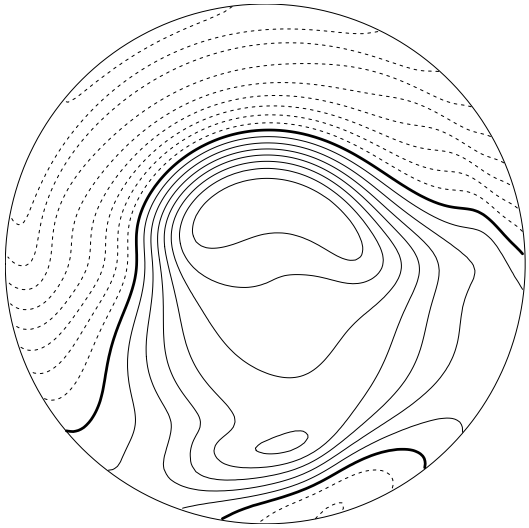

Figure 3. EPD resulting from a large anterior ischaemic region and a small posterior ischaemic region. (Min: -1.83mV, Max: 1.54mV)

points $(-3, 0, 0)$, $(3, 0, 0)$ and $(0, 0, 6)$. In each figure negative potentials are indicated by dashed lines, positive potentials by solid lines and the zero of potential by the thick solid line. The contour interval in each figure is 0.2mV.

As a baseline case, consider only one region of ischaemia, the EPD for which is shown in Figure 2. Here, the region of ischaemia is centred on the anterior of the ventricle and has an azimuthal range, θ, of 180° (ie $0° \leq \theta \leq 180°$) and a polar angle, ϕ, from 20° to 80°. The EPD shows ST-segment depression over much of the anterior and right sides of the ventricle towards the base. ST-elevation is observed over the apex and left-posterior of the epicardium. Such an EPD would produce a significant electrical dipole, which would be visible on an ECG.

Now consider the situation where there are two ischaemic regions, one large and one small. Figure 3 shows the EPD resulting from a large anterior ischaemic region (covering $0° \leq \theta \leq 180°$ and $20° \leq \phi \leq 80°$) and a small posterior region (covering $250° \leq \theta \leq 290°$ and $60° \leq \phi \leq 80°$). Here the EPD is very similar to the EPD shown in Figure 2 over the anterior surface and apex of the ventricle. Also, the range in potentials is not significantly different. In fact, the presence of this new ischaemic region appears to have very little effect on the zero and negative potential contour lines. However, over the posterior surface a small region of ST depression is observed. It is doubtful if this small change would be observable on an ECG.

In other simulations (results not shown), as the small posterior region of ischaemia moves more towards the apex, the small region of posterior ST depression also moves towards the apex, but becomes smaller in size and magnitude and eventually disappears. However, the pattern over the anterior surface and apex does not change significantly. Again, these changes would most likely not be visible on an ECG.

On the other hand, having two small regions of ischaemia can make significant differences to the EPD. Figure 4 shows the EPD resulting from an anterior ischaemic region $70° \leq \theta \leq 110°$ and $60° \leq \phi \leq 80°$ together with a posterior region $250° \leq \theta \leq 290°$ and $60° \leq \phi \leq 80°$. Note that two dipoles now appear on the epicardium. Note also, that the symmetric arrangement of ischaemic regions

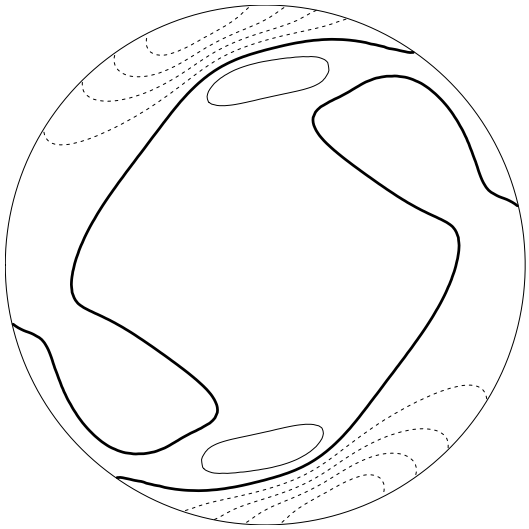

Figure 4. EPD obtained from two small ischaemic regions, one in the anterior and one in the posterior ventricular wall. (Min: -0.94mV, Max: 0.36mV)

gives rise to symmetric EPD patterns. These patterns change when the regions of ischaemia move. For example, moving the regions closer to the apex by reducing the polar angle brings the two dipole patterns closer together. Also, moving one ischaemic region from the anterior to the left of the ventricle, while leaving the posterior region unchanged, moves the top dipole pattern from Figure 4 towards the left of the EPD (Figure 5). However, these

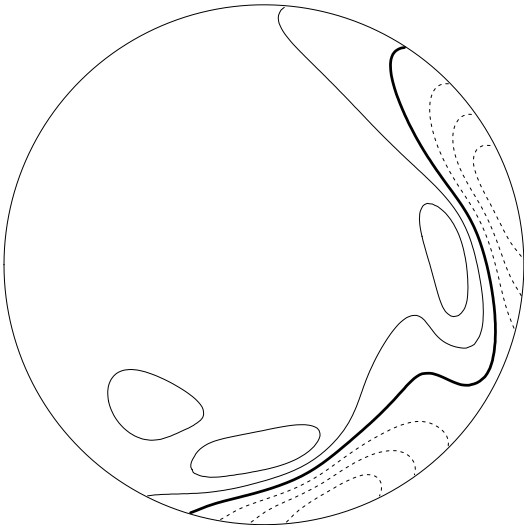

Figure 5. EPD obtained from two small ischaemic regions, one in the anterior and one in the left ventricular wall. (Min: -0.76mV, Max: 0.58mV)

smaller regions of ischaemia do not produce large potential gradients. Changes to patterns such as these might possible manifest themselves in the ECG.

4. Conclusions

This paper has considered an idealised model of the left ventricle with both one and two regions of subendocardial ischaemia. With two regions of ischaemia, one large anterior and one small posterior, the resulting EPD over the apex and anterior surface is not significantly different from the EPD resulting for one large anterior ischaemic region. Changing the position of the posterior region produces only minor changes in the EPD, which would most likely not be identifiable on an ECG. On the other hand, having two ischaemic regions of similar size is identifiable on the EPD and possibly on an ECG.

In the context of ST-segment counterpoise, it would appear that there are cancellation effects that were not demonstrated in the model presented. However, the changes brought about by considering multiple ischaemic regions are worthy of further study in a more realistic heart geometry and, perhaps, inside a torso model, instead of being considered in an isolated ventricular model.

References

[1] Madias JE. Ischaemic ST-segment counterpoise: One mechanism of false electrocardiographic response to exercise stress testing. American Jounral of Noninvasive Cardiology 1994;8:194–199.

[2] Madias JE, Mahjoub M, Valance J. The paradox of negative exercise stress ECG/positive thallium scintigram: ischemic ST-segment counterpoise as the underlying mechanism. Journal of Electrocardiology 1996;29(3):243–248.

[3] Madias JE, Khan M, Manyam B. The role of "ischemic ST-segment counterpoise" in rendering the response of exercise electrocardiogram falsely negative. Clinical Cardiology 1997;20:489–492.

[4] Hopenfeld B, Stinstra JG, MacLeod RS. The effect of conductivity on st-segment epicardial potentials arising from subendocardial ischemia. Annals of Biomedical Engineering 2005;33(6):751–763.

[5] Johnston PR. A finite volume method solution for the bidomain equations and their application to modelling cardiac ischaemia. Computer Methods in Biomechanics and Biomedical Engineering 2010;13(2):157–170.

[6] Gulrajani RM. Bioelectricity and Biomagnetism. New York: John Wiley and Sons, 1998.

[7] Potse M, Dubé B, Vinet A. Cardiac anisotropy in boundary-element models for the electrocardiogram. Medical Biological Engineering Computing 2009;47(7):719–729.

[8] Li D, Li CY, Yong AC, Kilpatrick D. Source of electrocardiographic ST changes in subendocardial ischemia. Circulation Research 1998;82:957–970.

[9] Clerc L. Directional differences of impulse spread in trabecular muscle from mammalian heart. Journal of Physiology 1976;255:335–346.

[10] Rush S, Abildskov JA, McFee R. Resistivity of body tissues at low frequencies. Circulation Research 1963;12:40–50.

[11] Tung L. A Bi–domain model for describing ischaemic myocardial D-C potentials. Ph.D. thesis, Massachusetts Institute of Technology 1978.

[12] Johnston PR, Kilpatrick D, Li CY. The importance of anisotropy in modelling ST segment shift in subendocardial ischaemia. IEEE Transactions on Biomedical Engineering 2001;48(12):1366–1376.

[13] Johnston PR, Kilpatrick D. The effect of conductivity values on ST segment shift in subendocardial ischaemia. IEEE Transactions on Biomedical Engineering 2003;50(2):150–158.

Address for correspondence:

Peter R. Johnston

School of Biomolecular and Physical Science, Griffith University, 170 Kessels Rd, Nathan, Queensland, Australia, 4111.

p.johnston@griffith.edu.au